Biochemical and Biophysical Research Communications 410 (2011) 189–194

Contents lists available at ScienceDirect

Biochemical and Biophysical Research Communications

journal homepage: www.elsevier.com/locate/ybbrc

Crystal structure of the cell corpse engulfment protein CED-2 in *Caenorhabditis elegans*

Yanyong Kang [a,b], Jing Xu [c], Yong Liu [a], Jian Sun [a], Dapeng Sun [a], Yingsong Hu [a], Yingfang Liu [a,*]

[a] National Laboratory of Biomacromolecules, Institute of Biophysics, Chinese Academy of Sciences, Beijing 100101, China
[b] Graduate University of the Chinese Academy of Sciences, Beijing 100049, China
[c] Key Laboratory of Molecular and Developmental Biology, Institute of Genetics and Developmental Biology, Chinese Academy of Sciences, Beijing, China

ARTICLE INFO

Article history:
Received 22 April 2011
Available online 17 May 2011

Keywords:
C. elegans
Cell corpse engulfment
CED-2
Crystal structure

ABSTRACT

In the nematode *Caenorhabditis elegans*, the cell corpse engulfment proteins CED-2, CED-5, and CED-12 act in the same pathway to regulate the activation of the Rac small GTPase, CED-10, leading to the rearrangement of the actin cytoskeleton for engulfing apoptotic cells. Nevertheless, it is not well understood how these proteins act together. Here we report the crystal structures of the CED-2 protein as determined by X-ray crystallography. The full-length CED-2 protein and its truncated form containing the N-terminal SH2 domain and the first SH3 domain show similar three-dimensional structures. A CED-2 point mutation (F125G) disrupting its interaction with the PXXP motif of CED-5 did not affect its rescuing activity. However, CED-2 was found to interact with the N-terminal region of CED-5. Our findings suggest that CED-2 may regulate cell corpse engulfment by interacting with CED-5 through the N-terminal region rather than the PXXP motif.

1. Introduction

Programmed cell death, or apoptosis, is an important cellular process that is conserved through evolution. When a cell begins apoptosis, it must be removed swiftly by engulfing cells. Defects in the clearance of apoptotic cells may trigger inflammatory or autoimmune diseases [1–3].

During the development of a hermaphrodite *Caenorhabditis elegans*, 131 of its total 1090 somatic cells undergo apoptosis [4]. Dying cells are quickly removed by neighboring cells, normally within one hour. Seven genes, *ced-1* (cell death abnormal), *ced-2*, *ced-5*, *ced-6*, *ced-7*, *ced-10*, and *ced-12*, were found by genetic studies to regulate the engulfment of cells undergoing programmed cell death [5–9]. When these genes are mutated, unengulfed cell corpses accumulate and can be distinguished as highly refractile disks under a Nomarski differential interference contrast (DIC) microscope. Further genetic analysis revealed that these genes act redundantly in two parallel pathways [4]. Proteins CED-1, CED-6, and CED-7 act in the same pathway to mediate and transduce cell-corpse engulfment signals [8–10], while CED-2, CED-5, and CED-12 (mammalian homologues CRKII, Dock180, and ELMO, respectively) form a complex to activate the GTPase CED-10 to regulate the actin cytoskeleton rearrangement, which is essential for cell migration and corpse engulfment [5,11–13].

CED-2 is a CRKII-like adaptor with one predicted SH2 domain at the N terminus followed by two consecutive SH3 domains at its C terminus. CED-5 is homologous to mammalian DOCK-180, a protein that was recently identified as a novel guanine nucleotide exchange factor (GEF) for small GTPases [11]. CED-2 can directly interact with CED-5, and the interaction is essential to the signaling of this engulfment pathway [11]. *ced-2* mutation results in defects in cell corpse engulfment [11]. It was reported previously that the first SH3 domain of CED-2 is essential for it to interact with the CED-5 C-terminal PXXP motif [14]. Moreover, deletion of the second SH3 domain in CED-2 also abolished its normal function [14,15]. Intriguingly, CED-5 lacking the CED-2-interacting PXXP motif was able to rescue the cell corpse engulfment defects in loss of *ced-5* mutants [16], raising the puzzle whether the interaction between CED-2 and CED-5 is essential for their functions in cell corpse engulfment.

To better understand the functional mechanism of CED-2 in the cell engulfment process, we used X-ray chromatography to determine the crystal structure of CED-2, from which we obtained detailed architectural information about this protein. We also identified CED-2 residues required for its interaction with CED-5 PXXP motif. Importantly, we found that CED-2 binds to CED-5 in addition to the PXXP motif. We suggest that, as an adaptor, CED-2 may recruit CED-5, through other part of CED-2 besides N-SH3

* Corresponding author.
E-mail address: liuy@ibp.ac.cn (Y. Liu).

0006-291X/$ - see front matter © 2011 Published by Elsevier Inc.
doi:10.1016/j.bbrc.2011.05.051

domain. Our results thus provide a platform for further study on the functional mechanism of CED-2/CED-5/CED-12 pathway.

2. Materials and methods

2.1. Cloning and mutagenesis

A 522-base pair DNA fragment, coding for residues 1–174 of *C. elegans* CED-2, was amplified from the full-length *ced-2* gene using the forward primer 5′-CCCCATATGCACCACCACCACCACCACATGACGACAAACGGG-3′ and the reverse primer 5′-CCGGAATTCTTACTGAATTTGTACATAG-3′, which contained restriction sites for *Nde*I and *Eco*RI, respectively. The resulting PCR product was inserted into vector pET21b (Novagen) for recombinant protein expression. A hexahistidine-tag coding sequence was included in the forward primer for protein purification. Full-length *ced-2* was similarly cloned into vectors pGEX-6p-1 and pET28a, which both have restriction enzyme sites for *Bam*HI and *Sal*I for GST-tagged or N-terminal His-tagged fusion protein expression. Several residues within these constructs were targeted for mutagenesis using the standard quick-change PCR method.

2.2. Protein expression and purification

The expression construct pET-21b-ced-2(1–174) was transformed into Rossetta II expression strains, and cultures were grown in LB medium at 37 °C to an A_{600} value of 0.6. Protein expression was induced by addition of isopropylthiogalactopyranoside (IPTG; 0.1 mM) for 18 h at 16 °C. Cells were harvested and resuspended in lysis buffer (20 mM Tris–Cl, pH 8.0, 150 mM NaCl, 10 mM imidazole) and then lysed by sonication. The lysate was centrifuged at 16,000*g* for 30 min, and the supernatant was collected. The soluble recombinant protein was then purified from cell supernatant by nickel-nitrilotriacetic acid chromatography (Qiagen) followed by gel filtration chromatography (Superdex200, Amersham Biosciences). The protein was concentrated in spin concentrators (Amicon, Millipore). SDS–PAGE was used to determine the purity of the proteins. The GST-fused CED-2 full-length protein was purified over a glutathione-Sepharose column, cleaved by PreScission, and further purified by gel filtration chromatography (Superdex 200, Amersham Biosciences).

2.3. Crystallization and data collection

The crystallization trials used the hanging-drop vapor diffusion method, mixing 1 μl of a protein solution with an equal volume of a reservoir solution using crystal screen kits. The best crystal of CED-2(1–174) was obtained in a solution containing 0.1 M HEPES-Na (pH 7.5) and 1.2 M lithium sulfate monohydrate. A mercury derivative was obtained by soaking the crystal in the presence of 0.1 mM $HgCl_2$. Native and derivative data sets were collected using an FR-E SuperBright rotating anode X-ray source equipped with an R-AXIS IV++ imaging plate detector (Rigaku). Data were collected at 150 K and processed using the HKL2000 program suite [17]. The crystals belonged to the $p6_122$ space group with cell dimensions of $a = b = 86.681$ Å and $c = 87.781$ Å, and there was one molecule per asymmetric unit.

The best crystals of full-length CED-2 were grown in a solution of 0.2 M lithium sulfate monohydrate, 0.1 M HEPES (pH 7.5), and 25% w/v polyethylene glycol 3350. Resolution was 2.5 Å and the space group was C2, different from that of CED-2(1–174).

2.4. Structure determination and refinement

The structure of CED-2(1–174) was solved by the method of single wavelength anomalous dispersion (SAD) using the mercury derivative data. The SHELXD program [18] was used and one Hg site was located; phasing was performed with the program suite PHENIX (Python-based Hierarchical Environment for Integrated Xtallography) [19]. The starting model was built into the density-modified electron density map using ARP/wARP [20]. The final model was obtained after iterative cycles of manual model building with COOT [21] and restrained refinement using REFMAC [22]. The final model contains 171 residues and 84 water molecules. The structure was refined to an R_{work} of 21.2% and an R_{free} of 27.6%. The atomic coordinates and diffraction data were deposited in the Protein Data Bank with the accession code 3QWX. The full-length CED-2 structure was solved by the method of molecular replacement by using the CED-2(1–174) structure as a searching model with Phaser [23]. The final structure was refined to an R_{work} of 21.5% and an R_{free} of 27.5%. The atomic coordinates and diffraction data were deposited in the Protein Data Bank with the accession code 3QWY All structural figures were prepared with PyMOL (http://www.pymol.org/). Crystallographic statistics are shown in Table 1.

2.5. In vitro binding assay

Two PXXP motifs (1716–1735 and 1759–1775) of CED-5 subcloned into the pGEX-6p-1 vector were expressed with an N-terminal GST tag. For a standard pull-down assay, GSH-Sepharose beads were added to supernatants that included both expressed GST-tagged CED-5 motifs and either His-tagged CED-2 or His-tagged CED-2 mutants. After incubation for 1 h at 4 °C, the resin was washed with PBS buffer three times. The GSH-Sepharose beads were resuspended and electrophoresed on SDS–PAGE.

Full-length GST-CED-2 and its mutants were expressed in *E. coli*. The *ced-5* cDNA fragments corresponding to amino acids 1–1414, 1415–1714, 1415–1781, as well as full-length CED-5 (1–1781), were subcloned into the pCITE-4a(+) vector (Novagen) and translated in the rabbit reticulocyte lysate (Promega) to obtain ^{35}S-methionine-labeled CED-5 protein. ^{35}S-labeled CED-5 was incubated with GST-CED-2, GST-CED-2 mutants, or GST alone for 2 h in PBS binding buffer. The resin was washed five times with 1 ml of binding buffer; the bound protein was separated by SDS–PAGE and visualized by autoradiography. Purified GST protein alone was used as a control.

2.6. C. elegans strains and genetics

To make *ced-2* rescuing construct, *ced-2* mutants and its truncations were amplified by polymerase chain reaction (PCR) and subsequently cloned into the vector pPD49.78 and pPD49.83 between the *Bam*HI and *Nco*I sites. We performed injections as previously described [24], using the pTG96 plasmid (20 μg/ml) as a co-injection marker. The pTG96 plasmid contains a *sur-5::gfp* fusion that is expressed in all somatic cells [25].

2.7. CED-2 rescuing experiments

We injected P_{hsp}ced-2 (40 μg/ml) with the co-injection marker pTG96 into *ced-2(n1994)* mutants to generate transgenic animals. We heat-shocked mixed-stage embryos at 33 °C for 1.5 h and then scored the number of cell corpses in 2.5-fold embryos about 4 h after the heat-shock treatment.

3. Results

3.1. Overall structure of CED-2

We first determined the crystal structure of the CED-2(1–174) fragment, which contains the N-terminal SH2 domain and the first

Table 1
Statistics from crystallographic analysis.

	CED-2 partial, native	CED-2 partial, $HgCl_2$ derivative	CED-2 full, native
Data collection			
Beamline	Rigaku FRE	Rigaku FRE	KEK BL5-A beamline[a]
Wavelength (Å)	1.5418	1.5418	1.0078
Space group	$P6_122$	$P6_122$	C1 2 1
Cell dimensions			
a, *b*, *c* (Å)	86.681, 86.681, 87.781	86.790, 86.790, 88.112	105.211, 97.152, 71.096
α, β, γ (°)	90.0, 90.0, 120.0	90.0, 90.0, 120.0	90.000, 127.137, 90.000
Resolution (outer shell), (Å)	50–2.01 (2.01–2.08)	50–2.42 (2.42–2.51)	50–2.5 (2.50–2.59)
R_{sym} (outer shell)	0.087 (0.482)	0.054 (0.132)	0.106 (0.610)
$I/\sigma I$ (outer shell)	32.8 (4.4)	52.7 (27.0)	23.8 (1.87)
Completeness (outer shell), (%)	99.9 (100.0)	99.6 (98.3)	99.6 (98.8)
Redundancy (outer shell)	11.2 (11.2)	11.3 (11.3)	4.2 (4.1)
Refinement			
Resolution (outer shell), (Å)	37.89–2.01 (2.01–2.08)		48.57–2.52 (2.50–2.59)
Total no. of reflection/free	13,490/667		18,916/965
R_{work}	0.212		0.215
R_{free}	0.276		0.275
No. of atoms			
Protein	1353		2691
Water	84		128
Ave. B-factors ($Å_2$)	26.97		56.88
R.m.s. deviations			
Bond lengths (Å)	0.008		0.009
Bond angle (°)	1.102		1.227
Ramachandran plot			
Favored (%)	97.5		95.2
Allowed (%)	2.5		3.3
Outlier (%)			1.5

$R_{sym} = \sum_h \sum i|I_{h,i} - I_h| \sum h \sum iI_{h,i}$, where I_h is the mean intensity of the *i* observations of symmetry-related reflections of $hR = |F_{obs} - F_{calc}| \sum F_{obs}$, where $F_{obs} = FP$, and F_{calc} is the calculated protein structure factor from the atomic model (R_{free} was calculated with 5% of the reflections). Root mean square deviation in bond lengths and angles are the deviations from ideal values.

[a] KEK: HIGH ENERGY ACCELERATOR RESEARCH ORGANIZATION, 1–1,KEK, Oho, Tsukuba, Ibaraki 305–0801 Japan.

SH3 domain (N-SH3) (Fig. 1A). The SH2 structure comprises residues 1–101, which form three α helices (α1–α3) and five β strands (β1–β5). The N-SH3 domain, comprising residues 118–174, consists of one short α helix (α4) and five β strands (β6–β10). The overall structures of these two domains are very similar to those of canonical SH2 and SH3 domains. These two domains are

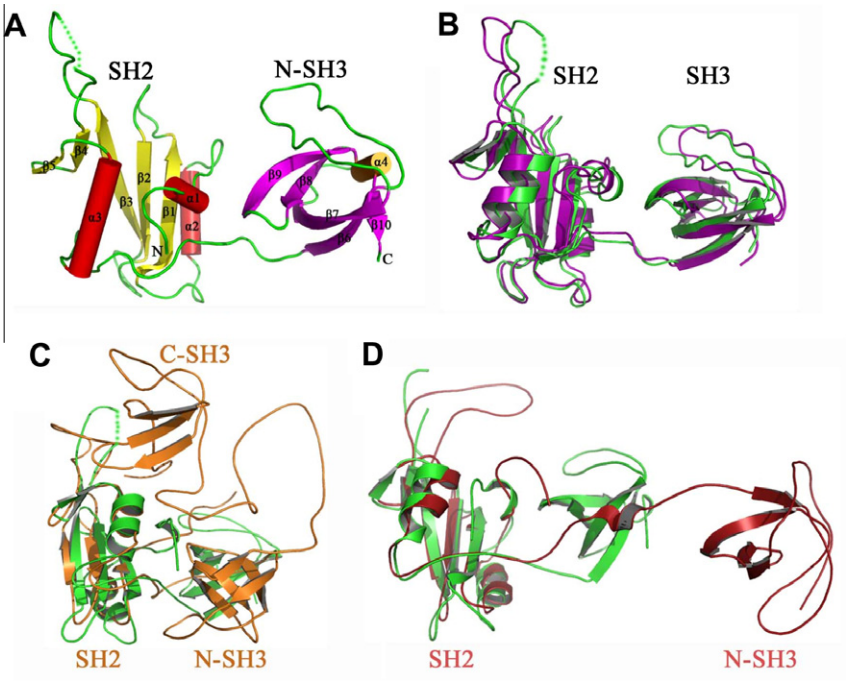

Fig. 1. Crystal structures of CED-2. (A) Structure of CED-2(1–174). SH2 domain (left) and the first SH3 domain (N-SH3) (right) are indicated. (B) Structure superposition of the CED-2(1–174) and the full-length CED-2; the density map of the latter only shows residues 1–174. Green represents CED-2(1–174), and magenta represents full-length CED-2. (C) Superposition of CED-2(1–174) (green) with full-length CRKII (yellow-orange). (D) Superposition of CED-2(1–174) (green) with CRKI (dark red). (For interpretation of the references to color in this figure legend, the reader is referred to the web version of this article.)

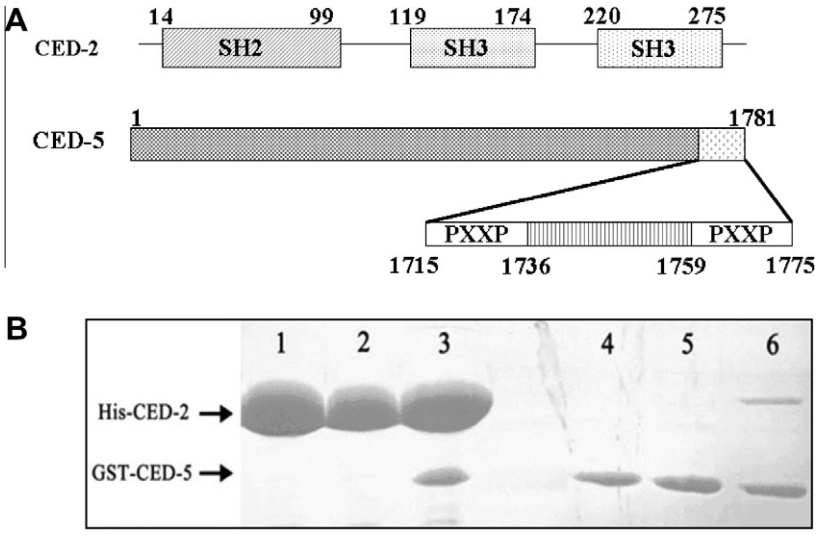

Fig. 2. Pull-down assay of His-tagged full-length CED-2 and GST-tagged CED-5(1715–1736) or GST-tagged CED-5(1759–1775). (A) schematic representation of both CED-2 and CED-5. (B) Nickel affinity beads pull down results: lane 1, His-CED-2 alone; lane 2, GST-CED-5(1715–1736) with His-CED-2; lane 3, GST-CED-5(1759–1775) with His-CED-2. GST beads pull down results: lane 4, GST -CED-5(1759–1775) alone; lane 5, GST-CED-5(1715–1736) with His-CED-2; lane 6, GST-CED-5(1759–1775) with His-CED-2.

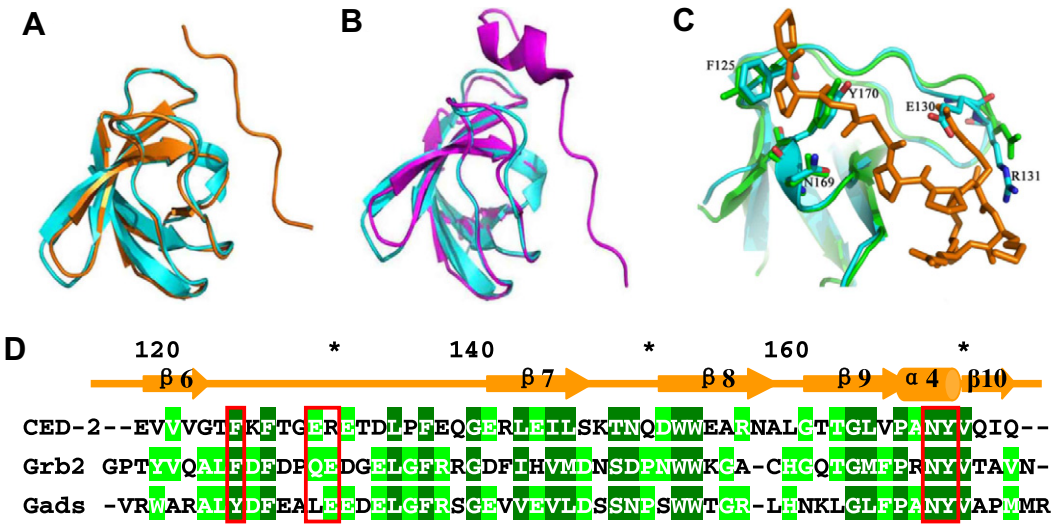

Fig. 3. Superposition of the CED-2 N-SH3 domain with that of (A) the GrB2-Gab2 complex and of (B) the Gads-HPK1 SH3C complex. The CED-2 N-SH3 domain is cyan, the GrB2 SH3 domain and Gab2 PXXP motif are orange, and the Gads SH3C and HPK1 PXXP motif are magenta. (C) Comparison of the CED-2 N-SH3 and Gads recognition residues for the PXXP motif. Side chains and structural elements from CED-2 and Gads are cyan and green, respectively. The PXXP motif of HPK1 is orange. (D) Sequence alignment of CED-2 N-SH3 with Grb2 and Gads. The red boxes show the residues that can interact with the CED-5 PXXP motif. Initial alignments were carried out using the ClustalW program. Completely conserved residues among these sequences are shaded in dark green, and residues conserved at least 70% percent are in light green. (For interpretation of the references to color in this figure legend, the reader is referred to the web version of this article.)

located side by side, yet there is no significant interaction between them. A long loop comprising residues 102–117 loosely links these two domains together.

We also purified and crystallized the full-length CED-2 protein. However, we failed to see the C-terminal SH3 domain in the electron density map, although the crystallized protein was still compact by mass spectrometry analysis (data not shown). We then performed a comparison of the two CED-2 structures to determine any differences between them (Fig. 1B). The overall structures of the two protein forms were almost the same. A small difference is that the crystal structure of the full-length CED-2 is slightly more extended than that of the CED-2 fragment (1–174).

CRKII, the homolog of CED-2 in humans, regulates transcription and cytoskeletal reorganization during cell growth, motility, proliferation, adhesion, differentiation, and apoptosis by acting as an adaptor that links tyrosine kinases and small G proteins. CRKI (SH2–SH3) and CRKII (SH2–SH3–SH3) are the two splicing isoforms. CRKI has higher fibroblast-transforming activity than CRKII. The reason for the higher activity is presumed to be that CRKI, without the third domain, has an open conformation in the cytoplasm and so can efficiently bind its effectors, including C3G, SOS, and Dock180. Subsequently, the effectors of CRK activate small G proteins that transmit signals to downstream molecules [26].

The similarity of the SH2 and N-SH3 structures in the two CED-2 forms we crystallized suggests that there is no significant conformational change when the C-terminal SH3 domain is deleted (Fig. 1B). However, the spatial locations of these two domains in CED-2 are significantly different than the locations of the comparable domains in CRKI. One possibility is that these two counterpart

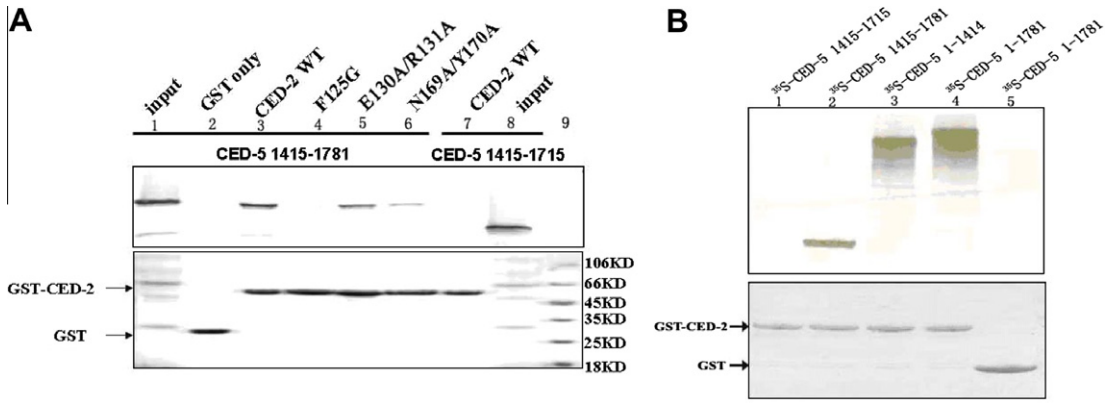

Fig. 4. In vitro binding Assay. (A) Autoradiograph results are in the upper panel. We used wild-type GST fused CED-2 or its mutants to pull-down ^{35}S-methionine-labeled CED-5(1415–1781) or CED-5(1415–1715). GST protein was used as a control. The final samples were applied to SDS–PAGE gel for autoradiographic analysis. Lanes 1 and 8 are the input of CED-5 for the assay, while lanes 3–7 are the results for the pull-down assay using CED-2 or mutants. Lane 2 is GST control. In the lower panel is the Coomassie blue staining result. Roughly equal amounts of GST-CED-2 and its mutants and the control GST protein were used in the binding reactions. Lane 9 is protein standard. B Autoradiography results (upper), CED-2 physically interact with CED-5 1415–1781 (line 2), CED-5 1–1414 (line 3) and CED-5 1–1781 (line 4), but not interact with CED-5 1415–1715 (line 1). GST shows no binding with full-length CED-5(1–1781) as a control (line 5). Lower. Equal CED-2 protein and GST protein were used for the binding assay.

proteins may have different structural arrangements; the second is that the proteins are flexible and the domain relative locations may change substantially under different conditions.

3.2. Identifying the CED-2 binding motif in the CED-5 C-terminus

The *ced-2*, *ced-5*, and *ced-12* genes are known to be required in the nematode *C. elegans* for efficient removal of apoptotic cell corpses. Previous studies have also shown that CED-2 can interact physically with the C-terminal PXXP motif of CED-5 [11,16]. There are two PXXP motifs, residues 1716–1735 and 1759–1775, at the CED-5 C-terminus. To determine which PXXP motif interacts with CED-2, we cloned them into bacterial expression vectors separately and purified them with an N-terminal GST fusion tag. Then we used *in vitro* pull-down experiments to test the binding affinity of these fusion proteins for purified recombinant full-length CED-2 protein. Our experiments showed that CED-2 was pulled down by the GST-fused CED-5(1759–1775) fragment (the second PXXP motif in CED-5), but not the CED-5(1715–1736) fragment (the first PXXP motif in CED-5) (Fig. 2).

3.3. Putative CED-5 PXXP motif binding revealed by sequence and structure comparisons

SH3 domains are found in many intracellular signaling proteins, and they mediate protein–protein interactions by binding to proline-rich peptide sequences. Some structures of SH3 in complex with proline-rich peptides have been determined previously, such as the Gads SH3C/HPK1 complex and the GrB2/Gab2 complex [27,28]. We compared our SH3 domain from CED-2 to those structures. Based on both sequence alignment and structural comparison, the CED-2 N-terminal SH3 domain is very similar to those in Gads SH3C and GrB2 [27,28] (Fig. 3A–D). We thus predicted that five residues of CED-2––F125, E130, R131, N169, and Y170—may be important for CED-2 binding to the CED-5 PXXP motif. To test our prediction, we prepared recombinant CED-2 mutant proteins and performed *in vitro* interaction experiments. We found that the F125G single mutation and the E130A/R131A and N169A/Y170A double mutations of CED-2 all significantly disrupted the binding affinity with the second PXXP motif of the CED-5 C-terminal (Fig. 4A).

To determine whether the binding of CED-2 to the PXXP motif of CED-5 is required for its function in cell corpse engulfment, we examined the rescuing activity of CED-2 mutant proteins in *ced-2* loss-of-function mutant worms. We found that CED-2 point mutations, F125G, E130A/R131A, and N169A/Y170A, which abolished or reduced CED-2 interaction with the CED-5 PXXP motif (Fig. 4A), exhibited the similar rescuing activity as the wild-type protein (Table 2), suggesting that CED-2 may not function through binding to the PXXP motif of CED-5. However, CED-2 mutant protein lacking the N-terminal SH2 domain (aa 1–174) or the C-terminal SH3 domain (113–279) failed to rescue the corpse engulfment defects in *ced-2* mutant worms.

Table 2
Rescue of cell corpse engulfment defect of the *ced-2* mutant by over-expression of wild-type *ced-2* and its mutants.

Transgene	Heat shock	No. of corpses	Range of cell corpses
None	–	21.0 ± 0.7	18–24
None	+	22.3 ± 0.7	17–25
P_{hsp}*ced-2-wt*	+	7.6 ± 0.5	4–14
	–	23.2 ± 0.8	18–31
P_{hsp}*ced-2-F125G*	+	5.7 ± 0.3	4–8
	–	22.8 ± 0.7	17–29
P_{hsp}*ced-2-E130A/R131A*	+	6.7 ± 0.4	4–11
	–	23.8 ± 0.8	17–30
P_{hsp}*ced-2-N169A/Y170A*	+	7.8 ± 0.5	5–13
	–	22.9 ± 0.6	20–31
P_{hsp}*ced-2-(1–174)*	+	24.9 ± 0.8	19–31
	–	22.4 ± 0.5	17–27
P_{hsp}*ced-2-(113–279)*	+	19.4 ± 0.9	16–27
	–	20.8 ± 0.8	17–28

At least three independent transgenic lines were scored and found to have similar results. The result from one line is shown. Number of cell corpses (mean ± SEM) was determined by Nomarski microscopy.

To further test if CED-2 can interact with CED-5 other than the PXXP motif, we performed *in vitro* binding between CED-2 with different truncations of CED-5. Although CED-2 did not interact with CED-5(1415–1715) which does not contain the PXXP motif, CED-2 could interact with CED-5(1–1414) (Fig. 4B), suggesting other CED-2 binding sites exist in CED-5, which might be important for the normal function of CED-2 and CED-5 in cell corpse engulfment.

4. Discussion

CED-2, CED-5, CED-12, and CED-10 were initially identified as part of the cell engulfment pathway, which removes apoptotic cells in the nematode *C. elegans*. CED-2 is an essential player in this

pathway and can interact with CED-5. The fact that CED-2 has three SH2/SH3 modules suggested that this protein may function as an adaptor to recruit other components for the pathway. From our structural information and biochemical analysis, we identified and confirmed that CED-2 interacts with the second PXXP motif (1759–1775) of CED-5 through residues in CED-2's N-SH3 domain. Previously, it was reported that deletion of PXXP motifs did not affect the rescuing activity of CED-5 in *ced-5* mutant worms [16], so they conclude that CED-2 binding sites on CED-5 are not required for engulfment and cell migration *in vivo*. Although our results also showed that disruption of the interaction between CED-2 and CED-5 C-terminal PXXP motifs did not affect CED-2 function in cell corpse engulfment, the most important finding from our studies is that CED-2 can interact with the N-terminal region of CED-5(1–1415). We also showed that deletion of the N-SH2 or C-SH3 domain abolished CED-2 function, which may play a very important role for the signaling or the interaction with other proteins. These results suggest that CED-2 and CED-5 may interact through other domains to achieve their functions in cell corpse removal.

CRKII is the CED-2 mammalian homolog protein; CRKI is a truncated version. CRKII has a lower transforming activity in cancer than CRKI. In CRKII, the binding sites of the SH2 domain for binding upstream signaling partners are masked by the C-SH3 domain, whereas CRKI has an extended open structure because the C-SH3 domain has been removed. For CED-2, deletion of the C-SH3 domain causes loss of cell engulfment signaling, although no obvious structural conformation changes in the first two domains are seen in our structures. This suggests that the way CED-2 regulates cell engulfment may be different from that of CRKII biological activity in human.

In summary, CED-2, CED-5, CED-12 and CED-10 were initially identified as part of the second genetic pathway in the nematode. Here we solved the crystal structure of CED-2, compared with the structure of mammalian homolog CrKI and CrKII, there are no major difference between full-length CED-2 and CED-2(1–174). Based on the structure, we concluded that the key residues for the interaction between CED-5 PXXP motifs and CED-2 N-SH3 domain, this interaction was not necessary for the corpse rescue is because that CED-2 interacts with other part of CED-5.

Acknowledgments

We thank Dr. Chonglin Yang from the Institute of Genetics and development for help with discussion and paper revision. We thank Jie Zhou for the help with structure determination. This work was supported by the Ministry of Science and Technology 863 Project (2006AA02A314), Ministry of Science and Technology 973 Project (2007CB914303 and 2011CB910300).

References

[1] J. Savill, Apoptosis in resolution of inflammation, J. Leukoc. Biol. 61 (1997) 375–380.
[2] N. Platt, R.P.da. Silva, S. Gordon, Recognizing death: the phagocytosis of apoptotic cells, Trends Cell Biol. 8 (1998) 365–372.
[3] D. Mevorach, The immune response to apoptotic cells, Ann. NY Acad. Sci. 887 (1999) 191–198.
[4] H.R. Horvitz, Nobel lecture Worms, life and death, Biosci. Rep. 23 (2003) 239–303.
[5] T.L. Gumienny, E. Brugnera, A.C. Tosello-Trampont, J.M. Kinchen, L.B. Haney, K. Nishiwaki, S.F. Walk, M.E. Nemergut, I.G. Macara, R. Francis, T. Schedl, Y. Qin, L. Van Aelst, M.O. Hengartner, K.S. Ravichandran, CED-12/ELMO, a novel member of the CrkII/Dock180/Rac pathway, is required for phagocytosis and cell migration, Cell 107 (2001) 27–41.
[6] R.E. Ellis, D.M. Jacobson, H.R. Horvitz, Genes required for the engulfment of cell corpses during programmed cell death in Caenorhabditis elegans, Genetics 129 (1991) 79–94.
[7] E.M. Hedgecock, J.E. Sulston, J.N. Thomson, Mutations affecting programmed cell deaths in the nematode Caenorhabditis elegans, Science 220 (1983) 1277–1279.
[8] Z. Zhou, E. Hartwieg, H.R. Horvitz, CED-1 is a transmembrane receptor that mediates cell corpse engulfment in *C. elegans*, Cell 104 (2001) 43–56.
[9] Y.C. Wu, H.R. Horvitz, The C. elegans cell corpse engulfment gene ced-7 encodes a protein similar to ABC transporters, Cell 93 (1998) 951–960.
[10] H.P. Su, K. Nakada-Tsukui, A.C. Tosello-Trampont, Y. Li, G. Bu, P.M. Henson, K.S. Ravichandran, Interaction of CED-6/GULP, an adapter protein involved in engulfment of apoptotic cells with CED-1 and CD91/low density lipoprotein receptor-related protein (LRP), J. Biol. Chem. 277 (2002) 11772–11779.
[11] P.W. Reddien, H.R. Horvitz, CED-2/CrkII and CED-10/Rac control phagocytosis and cell migration in *Caenorhabditis elegans*, Nat. Cell Biol. 2 (2000) 131–136.
[12] B. Conradt, Cell engulfment, No sooner ced than done, Dev. Cell 1 (2001) 445–447.
[13] Y.C. Wu, H.R. Horvitz, C. elegans phagocytosis and cell-migration protein CED-5 is similar to human DOCK180, Nature 392 (1998) 501–504.
[14] S. Akakura, B. Kar, S. Singh, L. Cho, N. Tibrewal, R. Sanokawa-Akakura, C. Reichman, K.S. Ravichandran, R.B. Birge, C-terminal SH3 domain of CrkII regulates the assembly and function of the DOCK180/ELMO Rac-GEF, J. Cell Physiol. 204 (2005) 344–351.
[15] P.M. Mangahas, Z. Zhou, Clearance of apoptotic cells in *Caenorhabditis elegans*, Semin. Cell Dev. Biol. 16 (2005) 295–306.
[16] A.C. Tosello-Trampont, J.M. Kinchen, E. Brugnera, L.B. Haney, M.O. Hengartner, K.S. Ravichandran, Identification of two signaling submodules within the CrkII/ELMO/Dock180 pathway regulating engulfment of apoptotic cells, Cell Death Differ. 14 (2007) 963–972.
[17] O. Z, M. W, Processing of X-ray diffraction data collected in oscillation mode, Meth. Enzymol. 276 (1997) 307–326.
[18] G.M. Sheldrick, in: S. Fortier (ed.), Direct Methods for Solving Macromolecular Structures, Kluwer Academic Publishers, Dordrecht, 1998, pp. 401–411.
[19] P.D. Adams, R.W. Grosse-Kunstleve, L.W. Hung, T.R. Ioerger, A.J. McCoy, N.W. Moriarty, R.J. Read, J.C. Sacchettini, N.K. Sauter, T.C. Terwilliger, PHENIX: building new software for automated crystallographic structure determination, Acta Crystallogr. D Biol. Crystallogr. 58 (2002) 1948–1954.
[20] A. Perrakis, R. Morris, V.S. Lamzin, Automated protein model building combined with iterative structure refinement, Nat. Struct. Biol. 6 (1999) 458–463.
[21] P. Emsley, K. Cowtan, Coot: model-building tools for molecular graphics, Acta Crystallogr. D Biol. Crystallogr. 60 (2004) 2126–2132.
[22] G.N. Murshudov, A.A. Vagin, E.J. Dodson, Refinement of macromolecular structures by the maximum-likelihood method, Acta Crystallogr. D Biol. Crystallogr. 53 (1997) 240–255.
[23] A.J. McCoy, R.W. Grosse-Kunstleve, P.D. Adams, M.D. Winn, L.C. Storoni, R.J. Read, Phaser crystallographic software, J. Appl. Crystallogr. 40 (2007) 658–674.
[24] C.C. Mello, J.M. Kramer, D. Stinchcomb, V. Ambros, Efficient gene transfer in C.elegans: extrachromosomal maintenance and integration of transforming sequences, EMBO J. 10 (1991) 3959–3970.
[25] T. Gu, S. Orita, M. Han, Caenorhabditis elegans SUR-5, a novel but conserved protein, negatively regulates LET-60 Ras activity during vulval induction, Mol. Cell Biol. 18 (1998) 4556–4564.
[26] Y. Kobashigawa, M. Sakai, M. Naito, M. Yokochi, H. Kumeta, Y. Makino, K. Ogura, S. Tanaka, F. Inagaki, Structural basis for the transforming activity of human cancer-related signaling adaptor protein CRK, Nat. Struct. Mol. Biol. 14 (2007) 503–510.
[27] M. Harkiolaki, T. Tsirka, M. Lewitzky, P.C. Simister, D. Joshi, L.E. Bird, E.Y. Jones, N. O'Reilly, S.M. Feller, Distinct binding modes of two epitopes in Gab2 that interact with the SH3C domain of Grb2, Structure 17 (2009) 809–822.
[28] M. Lewitzky, M. Harkiolaki, M.C. Domart, E.Y. Jones, S.M. Feller, Mona/Gads SH3C binding to hematopoietic progenitor kinase 1 (HPK1) combines an atypical SH3 binding motif, R/KXXK, with a classical PXXP motif embedded in a polyproline type II (PPII) helix, J. Biol. Chem. 279 (2004) 28724–28732.